International Journal of Engineering & Technology, 7 (4.26) (2018) 245-250

SPC

International Journal of Engineering & Technology

Website: www.sciencepubco.com/index.php/IJET

Research paper



Quantifying Tensile Properties of Bamboo Silicone Biocomposite using Yeoh Model

Kamarul Nizam Hassan[1], Jamaluddin Mahmud[2*], Anwar P.P. Abdul Majeed[3], Mohd Azman Yahaya[4]

[1]Faculty of Mechanical Engineering, Universiti Teknologi MARA, 40450 Shah Alam, Selangor, Malaysia
[2]Innovative Manufacturing, Mechatronics and Sports Laboratory, Faculty of Manufacturing Engineering, Universiti Malaysia Pahang, 26600 Pekan, Pahang, Malaysia
**Corresponding author E-mail: jm@salam.uitm.edu.my*

Abstract

The utilisation of bamboo has the potential of improving the properties of silicone. However, a thorough investigation has yet to be reported on the mechanical properties of bamboo silicone biocomposite. This study was carried out with the aim to quantify the tensile properties and assess the tensile behaviour of bamboo silicone biocomposite using Yeoh hyperelastic constitutive function. The specimens were prepared from the mix of bamboo particulate and pure silicone at various fibre composition ratio (0wt%, 1wt%, 3wt% and 5wt%) cured overnight at room temperature. A uniaxial tensile test was carried out by adopting the ASTM D412 testing standard. The Coefficient of Variation, CV, and the Coefficient of Determination, r^2, were determined to assess the reliability of the experimental data and fitting model. The results of the determined Yeoh material constants for 5wt% specimen is found to be $C_1 = 12.0603\times10^{-3}$ MPa, $C_2 = 8.7353\times10^{-5}$ MPa and $C_3 = -11.6165\times10^{-8}$ MPa, compared to pure silicone (0wt%) $C_1 = 5.6087\times10^{-3}$ MPa, $C_2 = 8.6639\times10^{-5}$ MPa and $C_3 = -7.6510\times10^{-8}$ MPa. The results indicate that the bamboo fibre improves the stiffness of the silicone rubber by 115 percent. A low variance was exhibited by the experimental data with a CV value of less than 8 percent. The Yeoh Model demonstrated an excellent prediction of the elastic behaviour of bamboo silicone biocomposite with a fitting accuracy of more than 99.93 percent.

Keywords: *Bamboo fibres; Hyperelastic; Tensile properties; Yeoh Model; Coefficient of Variation*

1. Introduction

The exploitation of natural fibers as reinforcement material has led to a massive development of biocomposite for various applications. The transition towards sustainable products is in tandem with one of the seventeen United Nation's Sustainable Development Goals that contribute towards a sustainable future. Lignocellulosic fibres possess an advantage over other natural fibres due to its massive annual production which reflected from substantial agriculture activities across the tropical continents especially in China, India and South East Asia [1-3]. These materials are favoured for their notable strength–to–density ratio and have been extensively utilised in the production of high–elastic–resistance and weight–reduced components for automobiles, aircraft, marines and buildings [4-11]. The integration can also be seen in the exploratory works of rubberlike composites, although the employment greatly accentuated on high–strength fibres such as jute and hemp [12-14]. The limitation, however, resulted in the diversity towards the exploration of alternative resources with comparable properties and yet, provide facile accessibility and less costly [15].

In Malaysia, bamboo offers considerable potential, primarily due to its large cultivation area and relatively cost-effective [16, 17]. It is worth to note that bamboo has identical performance to major timber species [18] and have been exploited in numerous form to cater for different industrial applications [19, 20]. Bamboo fibres are mostly incorporated into polymeric composites i.e. polyvinyl chloride (PVC) and high–density polyethylene (HDPE) where the addition enhances the stiffness and flexural strength of the matrixes [21, 22]. The integration was also found to improve the tensile modulus of natural rubber in [23, 24]. It is worth noting that the amount of fibre used was between 2.5 to 45 weight percent of the matrix. Though, the effect from the embedded fibre on elastomeric response has yet to be thoroughly reported in the previous work of rubber composites.

The characteristics of rubber, in contrary to bamboo fibre, are induced by the elastic behaviour of the material [25], hence, the need for nonlinear elastic models to quantify their properties is essential. Hyperelastic polynomial relations such as Neo–Hookean and Mooney–Rivlin are among the commonly used quantification models [26-30] owing to their lower degree of intricacy to be assessed as compared to exponential prediction models [31, 32]. However, the precision of the invariant–based models is limited by the presence of insufficient terms thus brought to the establishment of the extended polynomial hyperelastic models such as Yeoh and third order deformation approximation [33]. Yeoh model has been employed in many studies to quantify tensile [34], compressive [35] and shear [36] properties of rubberlike materials. The model was found to provide a reasonably accurate prediction of the experimental values with a relatively low error [37].

Therefore, this work attempts to quantify and assess the tensile properties of a novel bamboo silicone biocomposite using Yeoh hyperelastic constitutive equation. Low fibre loading was used to prevent the tendency for large size agglomerates to develop in the mixture [38]. The study also employed two different statistical indicators, namely, Coefficient of Variation, CV, and Coefficient of Determination, r^2 to assess the reliability of the attained experimental results and the prediction model respectively. Moreover, since silicone rubber is favoured in many applications, i.e.

Copyright © 2018 Authors. This is an open access article distributed under the Creative Commons Attribution License, which permits unrestricted use, distribution, and reproduction in any medium, provided the original work is properly cited.

biomedical and automotive, amongst others for its excellent material properties [30, 39, 40], thus interpreting its elastic response is of critical importance for design optimization.

2. Methodology

2.1. Specimen Formulation and Compounding

Bamboo acquired is of Dendrocalamus pendulus species with an initial moisture content of 36.5 percent. The culm was cut into sections before peeled and dried in an oven at 80^0 C for 24 h. Dried mid culm was then crushed using ball mill at a speed of 300 rpm for 2 h. The produced powder was ground using a 100 μm screen. Next, bamboo particulate and pure silicone (Ecoflex 0030) were mixed at a fibre composition ratio of 0, 1, 3 and 5 weight percentage to the matrix and left to cure overnight at room temperature. Specimens were labelled as BS00, BS01, BS03 and BS05 where the number represents the respective fibre composition. Composed specimens were considered to be homogeneous throughout the structure.

2.2. Tensile Test

The uniaxial tensile test was carried out using Shimadzu Autograph AG-X 5kN (Fig. 1), by employing the ASTM D412 testing standard [41]. A total of 20 specimens was tested; 5 specimens for every composition of bamboo particulate. Attained results were presented in the form of mean engineering stress–stretch relation.



Fig. 1: Tensile test in progress

2.3. Determining the Yeoh Material Constants

Mechanical properties of the composed material were determined numerically through the manipulation of Yeoh hyperelastic constitutive model to the experimental data. The general form of strain energy function is given by [33]:

$$W = C_{10}(I_1 - 3) + C_{20}(I_1 - 3)^2 + C_{30}(I_1 - 3)^3 \quad (1)$$

where C_{10}, C_{20} and C_{30} are the material constants of the tested specimen. For the case of incompressible material, the Green deformation tensor relation, I_1, reduces to:

$$I_1 = \lambda^2 + 2\lambda^{-1} \quad (2)$$

where λ is the principle extension ratio. Considering Piola Kirchhoff stress theory, engineering stress–stretch relation can be derived from Eq. (1):

$$\sigma_e = 2(\lambda - \lambda^{-2})(C_{10} + 2C_{20}(\lambda^2 + 2\lambda^{-1} - 3) + 3C_{30}(\lambda^2 + 2\lambda^{-1} - 3)^2) \quad (3)$$

Material constants were computed using the derivative of the polynomial regression method, which is represented by the following relation [42]:

$$S_r = \Sigma(\sigma(\lambda)_{i,\,exp} - \sigma(\lambda)_{i,\,model})^2 \quad (4)$$

This method has been employed in various studies due to its effectiveness in solving multiple–constant polynomial equation [43, 44].

2.4. Statistical Analysis

The precision of the experimental results was measured by the evaluation of data extendibility using Coefficient of Variation relation [45]:

$$CV = [\Sigma(\lambda_i - \lambda_{mean})^2 / (n - 1)]^{1/2} / |\lambda_{mean}| \quad (5)$$

where n is the number of specimens. In general, the value of CV represents the ratio of sample standard deviation relative to its absolute mean, λ_{mean} at predetermined stress magnitude. A dataset of high precision scattered at low variance, contributed to the small CV value vice versa [46, 47].
Moreover, the accuracy of the fitted curves was determined using the Coefficient of Determination (COD) relation [42]:

$$r^2 = 1 - \Sigma(\sigma(\lambda)_{i,\,exp} - \sigma(\lambda)_{i,\,model})^2 / \Sigma(\sigma(\lambda)_{i,\,exp} - \sigma(\lambda)_{mean})^2 \quad (6)$$

Mainly, the higher coefficient value indicates higher accuracy is achieved by the prediction model to the original uncertainties of experimental data [48, 49].

3. Results and Discussion

Fig. 2 shows the uniaxial elastic behaviour of bamboo silicone biocomposite at various fibre–to–matrix ratio. All curves display nonlinear characteristic in which similar to the profile of silicone rubber composites reported in [30, 50].

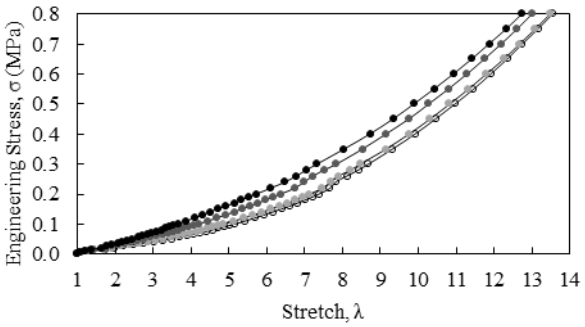

Fig. 2: Mean stress–stretch behaviour of specimens BS00 (○); BS01 (●); BS03 (●); and BS05 (●).

It is interesting to note the transition of the curvilinear trend across the axes. It could be observed that the addition of bamboo filler into the silicone rubber matrix affects the elasticity properties of

the developed biocomposite. This is apparent with the decrease in the elongation of 6 percent. A similar trend was also portrayed in [50] where the relative strain reduces with the increase of fibre content. The poor elasticity behaviour is resulted from the progression of strain energy, which leads to a higher degree of resistance of the structure towards large deformation state.

Furthermore, it could also be observed that along the deformation range $2 \leq \lambda \leq 7$, gradual increment transpired to the slope of the curves which suggested that stiffening effect is highly intensified at lower stress range (20 kPa $\leq \sigma \leq$ 300 kPa). The presence of more fillers provides a larger surface area, allowing higher load transfer to take place due to the significant interaction occurs between matrix and fibres [39, 51]. The increase in stiffness is reflected by the upsurge trend of constant C_1 in Table 1. The stiffness of the silicone rubber was found to enhance by 115 percent with the incorporation of 5 wt% bamboo fibres. The elongation profile also tends to be less nonlinear in which conveyed by the decreasing value of constant C_3. However, no changes transpired to the behaviour of the stress–stretch curve beyond the aforesaid range, probably due to the greater matrix crosslinking effect as compared to the fibre reinforcing [24]. Such occurrence can be related to the unvarying trend of the constant C_2 in the presented table.

Table 1: Yeoh material constants determined at various composition

Specimens	Fibre Addition (wt%)	Material Constants (MPa)			COD, r^2
		C_1 (10^{-3})	C_2 (10^{-5})	C_3 (10^{-8})	
BS00	0	5.6087	8.6639	-7.6510	0.9998
BS01	1	6.6271	8.6510	-8.3200	0.9999
BS03	3	9.3171	9.0450	-10.7941	0.9997
BS05	5	12.0603	8.7353	-11.6165	0.9993

Fig. 3 shows the CV value of the experimental data at various mean stretch. High CV value was found to appear in the range of $2 \leq \lambda \leq 7$ which concentred at 200 percent stretch for all specimens. The emergence of the peak value is brought by the abrupt data distribution exhibited by the specimens within the stress value of 0.02 to 0.03 MPa (refer Fig. 4). However, as the exerted load increases, the transpired elongation becomes closer to the sample mean, that in turn resulted in the less deviation of the error bar. Despite the broad data distribution exhibited in Fig. 4(c) and 4(d), low variance data appeared in the stress–stretch diagram of specimens BS00 and BS01 with a CV value of less than 3 percent (Fig. 4(a) and 4(b)).

In terms of reinforcing mechanism, such development might be associated to the disproportionate tensile strength exhibited by the distinctive specimens as a result from the presence of the large and poor dispersion of agglomerates throughout the matrix [52-54]. The development of the filler network during low deformation is highly related to the higher surface interaction between fibre and matrix [55]. However, as the concentration of filler increases, the matrix–filler interaction tends to become weaker due to the reduction of specific surface area transpired from the agglomeration of fibres [56]. Large agglomerates act as a stress concentrator in a matrix [56] and it is unfavoured for its low transverse stiffness [48]. Agglomerates with a size larger than the flaw size of matrix contribute to poor dispersion [57, 58] and deteriorate the mechanical properties [54].

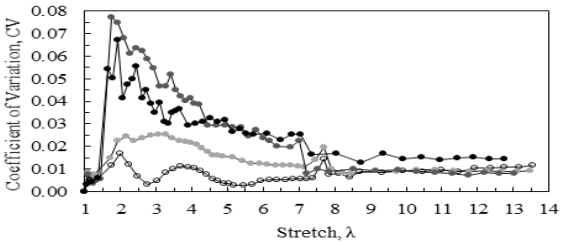

Fig. 3: Coefficient of variation of dataset attribute to specimens BS00 (○); BS01 (●); BS03 (●); and BS05 (●) at various mean stretch

Though, less variation was found to appear to the data set beyond 700 percent stretch range with a CV value of less than 2 percent. At large strain, filler network tends to be weak due to amplification of local strain which causes rubber chains between crosslinks to greatly extend [55]. The development of rubber crosslinking reduces the inconsistency of reinforcing effect thus resulted in the homogeneous deformation of the specimens. All the data attained from the experiment are distributed within 95 percent of the normal distribution.

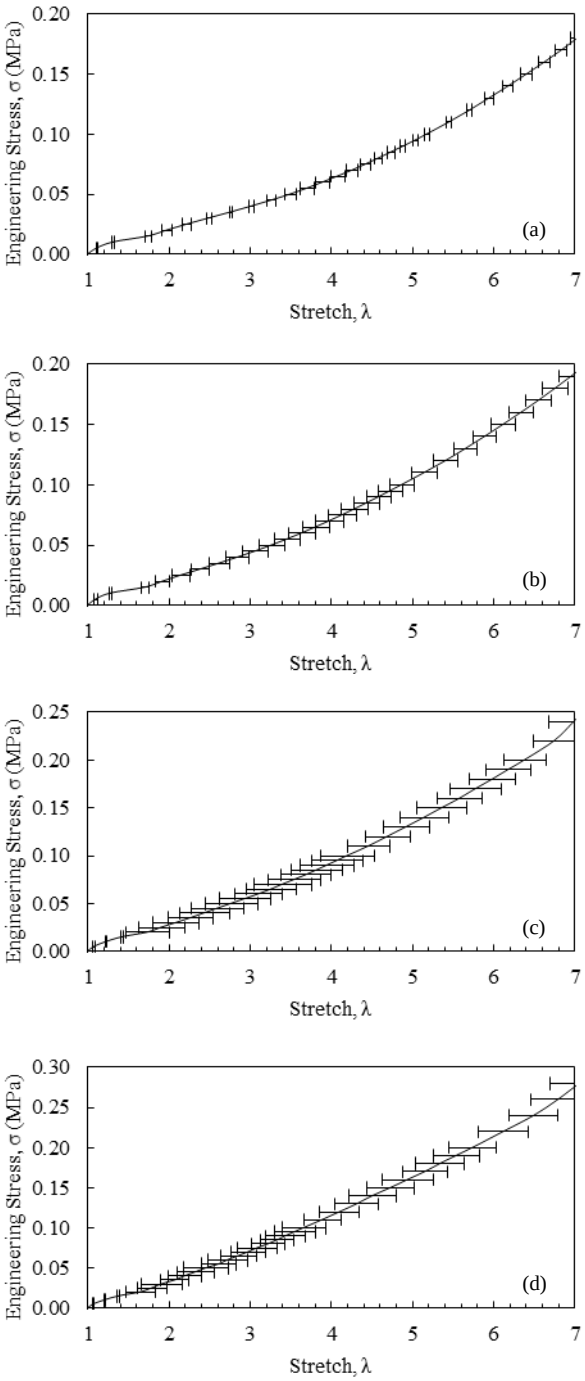

Fig. 4: Mean stress–stretch behaviour of specimens (a) BS00; (b) BS01; (○) BS03; and (d) and BS05 focusing specifically on deformation region of $1 \leq \lambda \leq 7$ with 2 standard deviation error bar.

The stress–stretch curve for each variation is separated into Fig. 5(a), Fig. 5(b), Fig 5(c) and Fig 5(d) to explicitly highlight the behaviour of the prediction curve (Yeoh Model) with respect to the experimental value. Predicted hyperelastic profiles are depicted by the dashed curve lines. The fitted curves are almost consistent with the experimental data value (denoted by markers) with

a standard error of less than 1 percent. The high value of r^2 obtained indicates the adequacy of the Yeoh Model on representing the experimental results. The outcome shows that there is a real relation between stretch, λ, and stress, σ, [43] for all tested specimens in present work.

Nevertheless, at lower stretch range ($1 \leq \lambda \leq 3.25$), a high discrepancy occurs to the projections (Fig. 6(a) to 6(d)) due to the inherent limitation of the model on depicting small strain behaviour of large deformation material [33]. Disassociation of invariant tensor I_2 has brought to such drawback [33]. A relative error within the range was found to be 31.38, 30.27, 34.09 and 56.42 percent which attribute to the prediction model of specimen BS00, BS01, BS03 and BS05 respectively. An inverse relation can be seen between relative error and coefficient of determination value – the higher the error transpired, the lower the value of the coefficient attained. At higher stretch range ($3.25 < \lambda \leq 14$), transpired relative error is below 5 percent for all predicted value.

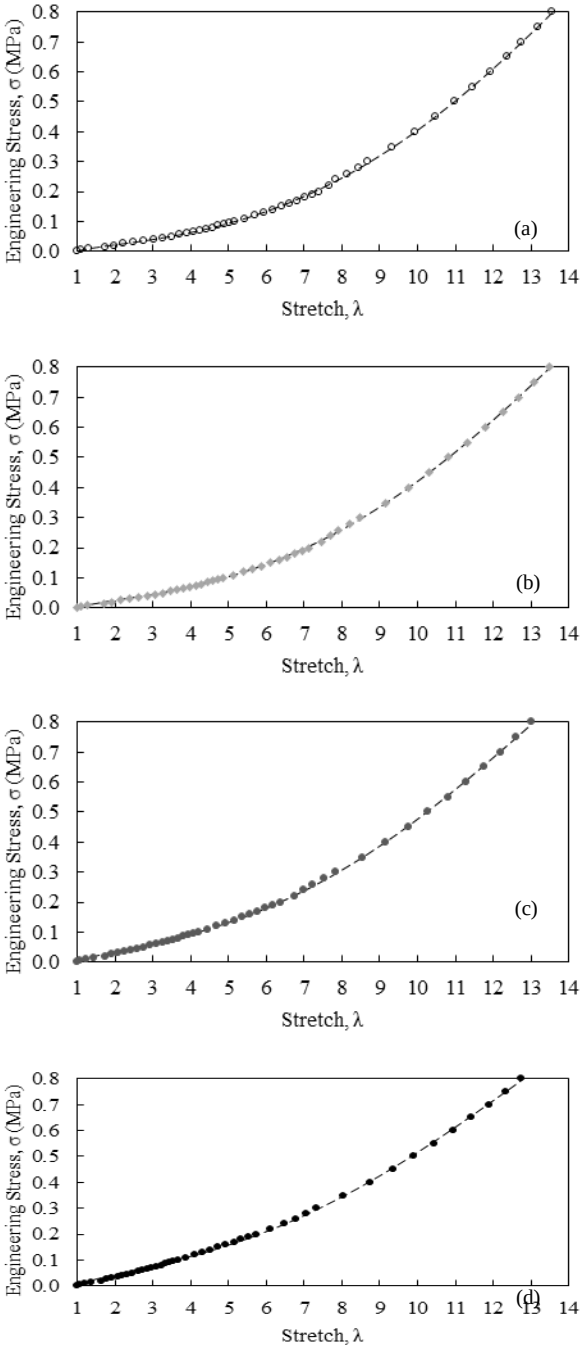

Fig. 5: Mean stress–stretch behaviour of specimens (a) BS00; (b) BS01; (c) BS03; and (d) BS05 and respective Yeoh Model prediction curves.

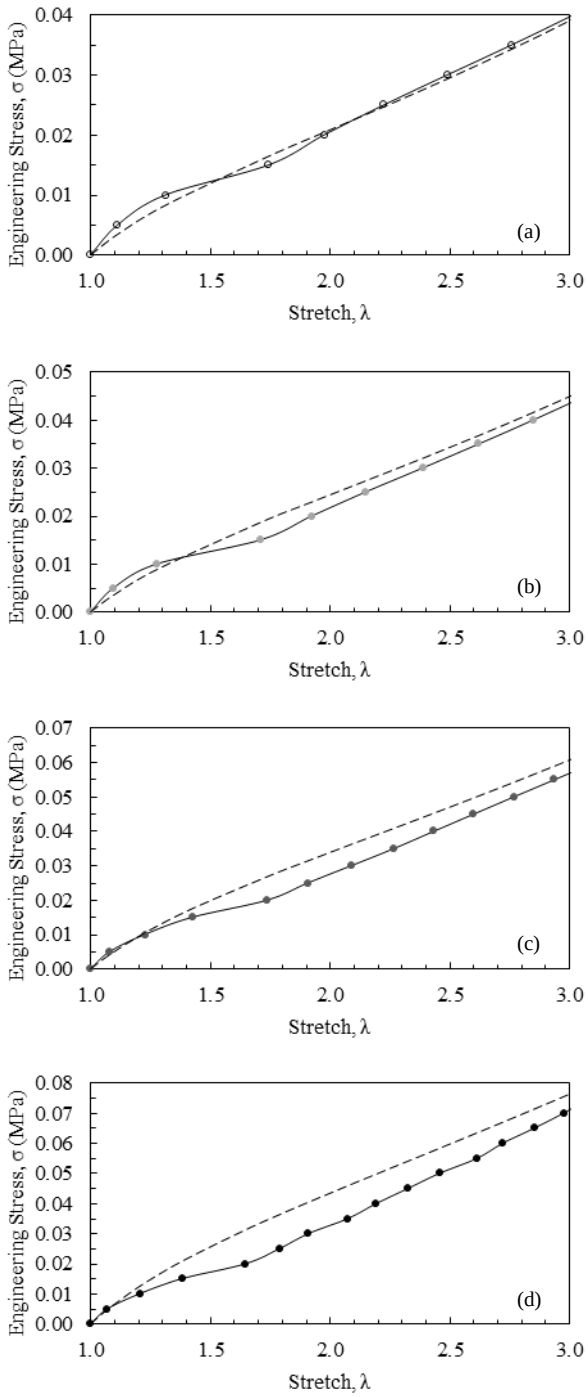

Fig. 6: Mean stress–stretch behaviour of specimens (a) BS00; (b) BS01; (c) BS03; and (d) BS05 in deformation region of $1 \leq \lambda \leq 3$. The dashed line represents the Yeoh Model prediction curve.

4. Conclusion

This paper reports the work related to the quantification of the tensile properties of bamboo silicone biocomposite. The variation of experimental data was found to be acceptable with the distribution of less than 8 percent. It was observed that the stiffness of bamboo silicone biocomposite is improved by 115 percent through the reinforcement of 5 weight percent ratio of bamboo fibres into silicone rubber. Moreover, an excellent prediction of the elastic behaviour of tested specimens was demonstrated by the Yeoh Model, suggesting its efficacy in predicting the behaviour of the proposed biocomposite. Future works will involve the investigation and the quantification of the compressive behaviour of

bamboo reinforced silicone biocomposite to provide further insight on its potentiality and practical implications.

Acknowledgement

The authors gratefully acknowledge the financial support by the Ministry of Higher Education Malaysia (MOHE) and Universiti Teknologi MARA (UiTM). (Grant no: 600–RMI/FRGS 5/3 (0098/2016))

References

[1] Yan L, Kasal B, and Huang L (2016), A review of recent research on the use of cellulosic fibres, their fibre fabric reinforced cementitious, geo-polymer and polymer composites in civil engineering, *Composites Part B: Engineering*, Vol. 92, 94-132.

[2] Shah DU, Porter D, and Vollrath F (2014), Can silk become an effective reinforcing fibre? A property comparison with flax and glass reinforced composites, *Composites Science and Technology*, Vol. 101, 173-183.

[3] Du Y, Yan N, and Kortschot MT (2015), The use of ramie fibers as reinforcements in composites, 104-137.

[4] Pickering KL, Efendy MGA, and Le TM (2016), A review of recent developments in natural fibre composites and their mechanical performance, *Composites Part A: Applied Science and Manufacturing*, Vol. 83, 98-112.

[5] Kong C, Lee H, and Park H (2016), Design and manufacturing of automobile hood using natural composite structure, *Composites Part B: Engineering*, Vol. 91, 18-26.

[6] Omrani E, Menezes PL, and Rohatgi PK (2016), State of the art on tribological behavior of polymer matrix composites reinforced with natural fibers in the green materials world, *Engineering Science and Technology, an International Journal*, Vol. 19, 717-736.

[7] Alkbir MFM, Sapuan SM, Nuraini AA, and Ishak MR (2016), Fibre properties and crashworthiness parameters of natural fibre-reinforced composite structure: A literature review, *Composite Structures*, Vol. 148, 59-73.

[8] Castegnaro S, Gomiero C, Battisti C, Poli M, Basile M, Barucco P, *et al.* (2017), A bio-composite racing sailboat: Materials selection, design, manufacturing and sailing, *Ocean Engineering*, Vol. 133, 142-150.

[9] Balakrishnan P, John MJ, Pothen L, Sreekala MS, and Thomas S (2016), Natural fibre and polymer matrix composites and their applications in aerospace engineering, 365-383.

[10] Page J, Khadraoui F, Boutouil M, and Gomina M (2017), Multi-physical properties of a structural concrete incorporating short flax fibers, *Construction and Building Materials*, Vol. 140, 344-353.

[11] Onuaguluchi O and Banthia N (2016), Plant-based natural fibre reinforced cement composites: A review, *Cement and Concrete Composites*, Vol. 68, 96-108.

[12] Nair AB and Joseph R (2014), Chemistry, Manufacture and Applications of Natural Rubber, *Woodhead Publishing*, pp. 249-283.

[13] Nunes RCR (2014), Chemistry, Manufacture and Applications of Natural Rubber, *Woodhead Publishing*, pp. 284-302.

[14] Adekomaya O, Jamiru T, Sadiku R, and Huan Z (2017), Negative impact from the application of natural fiber, *Journal of Cleaner Production*, Vol. 143, 843-846.

[15] Dittenber DB and GangaRao HVS (2012), Critical review of recent publications on use of natural composites in infrastructure, *Composites Part A: Applied Science and Manufacturing*, Vol. 43, 1419-1429.

[16] Bahari SA and Krause A (2016), Utilizing Malaysian bamboo for use in thermoplastic composites, *Journal of Cleaner Production*, Vol. 110, 16-24.

[17] Gurunathan T, Mohanty S, and Nayak SK (2015), A review of the recent developments in biocomposites based on natural fibres and their application perspectives, *Composites Part A: Applied Science and Manufacturing*, Vol. 77, 1-25.

[18] Ahmad M and Kamke FA (2005), Analysis of Calcutta bamboo for structural composite materials: physical and mechanical properties, *Wood Science and Technology*, Vol. 39, 448-459.

[19] Sharma B, Gatóo A, Bock M, and Ramage M (2015), Engineered bamboo for structural applications, *Construction and Building Materials*, Vol. 81, 66-73.

[20] Kumar A, Vlach T, Laiblova L, Hrouda M, Kasal B, Tywoniak J, *et al.* (2016), Engineered bamboo scrimber: Influence of density on the mechanical and water absorption properties, *Construction and Building Materials*, Vol. 127, 815-827.

[21] Qian SP, Wang H, Zarei E, and Sheng KC (2015), Effect of hydrothermal pretreatment on the properties of moso bamboo particles reinforced polyvinyl chloride composites, *Composites Part B-Engineering*, Vol. 82, 23-29.

[22] Wang C, Wang S, Cheng H, Xian Y, and Zhang S (2017), Mechanical properties and prediction for nanocalcium carbonate-treated bamboo fiber/high-density polyethylene composites, *Journal of Materials Science*, Vol. 52, 11482-11495.

[23] Ismail H, Edyham MR, and Wirjosentono B (2002), Bamboo fibre filled natural rubber composites: the effects of filler loading and bonding agent, *Polymer Testing*, Vol. 21, 139-144.

[24] Visakh PM, Thomas S, Oksman K, and Mathew AP (2012), Crosslinked natural rubber nanocomposites reinforced with cellulose whiskers isolated from bamboo waste: Processing and mechanical/thermal properties, *Composites Part A: Applied Science and Manufacturing*, Vol. 43, 735-741.

[25] Gent AN (2013), The Science and Technology of Rubber, 4 ed. *Academic Press*, Boston, pp. 1-26.

[26] Sasso M, Palmieri G, Chiappini G, and Amodio D (2008), Characterization of hyperelastic rubber-like materials by biaxial and uniaxial stretching tests based on optical methods, *Polymer Testing*, Vol. 27, 995-1004.

[27] Bailly L, Toungara M, Orgeas L, Bertrand E, Deplano V, and Geindreau C (2014), In-plane mechanics of soft architectured fibre-reinforced silicone rubber membranes, *J Mech Behav Biomed Mater*, Vol. 40, 339-53.

[28] Yang H, Yao X-F, Ke Y-C, Ma Y-j, and Liu Y-H (2016), Constitutive behaviors and mechanical characterizations of fabric reinforced rubber composites, *Composite Structures*, Vol. 152, 117-123.

[29] Chen L, Jia Z, Tang Y, Wu L, Luo Y, and Jia D (2017), Novel functional silica nanoparticles for rubber vulcanization and reinforcement, *Composites Science and Technology*, Vol. 144, 11-17.

[30] Bernardi L, Hopf R, Ferrari A, Ehret AE, and Mazza E (2017), On the large strain deformation behavior of silicone-based elastomers for biomedical applications, *Polymer Testing*, Vol. 58, 189-198.

[31] Ogden RW (1972), Large Deformation Isotropic Elasticity - On the Correlation of Theory and Experiment for Incompressible Rubberlike Solids, *Proceedings of the Royal Society A: Mathematical, Physical and Engineering Sciences*, Vol. 326, 565-584.

[32] Mahmud J, Holt CA, Evans SL, and Manan NFA (2013), Quantifying Skin Properties Using a Novel Integration Experiment-Finite Element Simulation and Skin Pre-Stretch Model, *Advanced Science Letters*, Vol. 19, 3155-3160.

[33] Yeoh OH (1990), CHARACTERIZATION OF ELASTIC PROPERTIES OF CARBON-BLACK-FILLED RUBBER VULCANIZATES, *Rubber Chemistry and Technology*, Vol. 63, 792-805.

[34] Karimi A, Navidbakhsh M, and Beigzadeh B (2014), A visco-hyperelastic constitutive approach for modeling polyvinyl alcohol sponge, *Tissue Cell*, Vol. 46, 97-102.

[35] Dispersyn J, Hertelé S, Waele WD, and Belis J (2017), Assessment of hyperelastic material models for the application of adhesive point-fixings between glass and metal, *International Journal of Adhesion and Adhesives*, Vol. 77, 102-117.

[36] Benevides RO and Nunes LCS (2015), Mechanical behavior of the alumina-filled silicone rubber under pure shear at finite strain, *Mechanics of Materials*, Vol. 85, 57-65.

[37] Mansouri MR and Darijani H (2014), Constitutive modeling of isotropic hyperelastic materials in an exponential framework using a self-contained approach, *International Journal of Solids and Structures*, Vol. 51, 4316-4326.

[38] Vijayan D, Mathiazhagan A, and Joseph R (2017), Aluminium trihydroxide: Novel reinforcing filler in Polychloroprene rubber, *Polymer*, Vol. 132, 143-156.

[39] Ziraki S, Zebarjad SM, and Hadianfard MJ (2016), A study on the tensile properties of silicone rubber/polypropylene fibers/silica hybrid nanocomposites, *J Mech Behav Biomed Mater*, Vol. 57, 289-96.

[40] Guo L, Lv Y, Deng Z, Wang Y, and Zan X (2016), Tension testing of silicone rubber at high strain rates, *Polymer Testing*, Vol. 50, 270-275.

[41] Azmi NN, Patar MNAA, Noor SNAM, and Mahmud J (2014), Testing standards assessment for silicone rubber, *2014 International Symposium on Technology Management and Emerging Technologies*, pp. 332-336.
[42] Chapra SC and Canale RP (2015), Numerical Methods for Engineers, 7th ed. *McGraw-Hill Education*, New York, pp. 472-475.
[43] Gendy TS, El-Shiekh TM, and Zakhary AS (2015), A polynomial regression model for stabilized turbulent confined jet diffusion flames using bluff body burners, *Egyptian Journal of Petroleum*, Vol. 24, 445-453.
[44] Ostertagová E (2012), Modelling using Polynomial Regression, *Procedia Engineering*, Vol. 48, 500-506.
[45] Reh W and Scheffler B (1996), Significance tests and confidence intervals for coefficients of variation, *Computational Statistics & Data Analysis*, Vol. 22, 449-452.
[46] Bruderer R, Bernhardt OM, Gandhi T, Xuan Y, Sondermann J, Schmidt M, *et al.* (2017), Optimization of Experimental Parameters in Data-Independent Mass Spectrometry Significantly Increases Depth and Reproducibility of Results, *Mol Cell Proteomics*, Vol. 16, 2296-2309.
[47] Bąkowski A, Radziszewski L, and Žmindak M (2017), Analysis of the Coefficient of Variation for Injection Pressure in a Compression Ignition Engine, *Procedia Engineering*, Vol. 177, 297-302.
[48] Joffre T, Miettinen A, Wernersson ELG, Isaksson P, and Gamstedt EK (2014), Effects of defects on the tensile strength of short-fibre composite materials, *Mechanics of Materials*, Vol. 75, 125-134.
[49] Lee SH, Goddard ME, Wray NR, and Visscher PM (2012), A better coefficient of determination for genetic profile analysis, *Genet Epidemiol*, Vol. 36, 214-24.
[50] Berahman R, Raiati M, Mehrabi Mazidi M, and Paran SMR (2016), Preparation and characterization of vulcanized silicone rubber/halloysite nanotube nanocomposites: Effect of matrix hardness and HNT content, *Materials & Design*, Vol. 104, 333-345.
[51] Väisänen T, Das O, and Tomppo L (2017), A review on new bio-based constituents for natural fiber-polymer composites, *Journal of Cleaner Production*, Vol. 149, 582-596.
[52] Zhang D, He M, Qin S, and Yu J (2017), Effect of fiber length and dispersion on properties of long glass fiber reinforced thermoplastic composites based on poly(butylene terephthalate), *RSC Advances*, Vol. 7, 15439-15454.
[53] De Paoli MA, Pure IUo, and Division ACM (2002), Polymer Science Insights, *Wiley*.
[54] Cheremisinoff NP and Cheremisinoff PN (1996), Handbook of Applied Polymer Processing Technology, *Taylor & Francis*.
[55] Sahakaro K (2017), Progress in Rubber Nanocomposites, *Woodhead Publishing*, pp. 81-113.
[56] Atif R and Inam F (2016), Reasons and remedies for the agglomeration of multilayered graphene and carbon nanotubes in polymers, *Beilstein Journal of Nanotechnology*, Vol. 7, 1174-1196.
[57] Litster J (2016), Design and Processing of Particulate Products, *Cambridge University Press*.
[58] Beaumont PWR, Soutis C, and Hodzic A (2016), The Structural Integrity of Carbon Fiber Composites: Fifty Years of Progress and Achievement of the Science, Development, and Applications, *Springer International Publishing*.